Numerical parametric evaluation of ultimate resistance of high-strength bolts

Li, Jie; Xin, Haohui; Wang, Zhiqiang; Veljkovic, Milan; Bingzhen, Zhao; Zhao, Junjie; Correia, José A.F.O.

Important note
To cite this publication, please use the final published version (if applicable).
Please check the document version above.

Numerical parametric evaluation of ultimate resistance of high-strength bolts

Jie Li [a], Haohui Xin [a,*], Zhiqiang Wang [b], Milan Veljkovic [c], Zhao Bingzhen [b], Junjie Zhao [b], José A.F.O. Correia [d]

[a] Department of Civil Engineering, Xi'an Jiaotong University, Xi'an 710116, China
[b] Shaanxi Construction Engineering Holding Group, Xi'an 710116, China
[c] Faculty of Civil Engineering and Geosciences, Delft University of Technology, Netherlands
[d] Department of Civil Engineering, University of Porto, Portugal

A B S T R A C T

High strength bolts are widely used in the engineering field due to their good compressive properties. Accurate assessment of the ultimate capacity performance of high strength bolts under combined loading is essential to ensure the safety of steel structures in the connection zone. Existing studies are not sufficiently clear on the economic and condition-specific limits on the effects of various factors on high-strength bolts under complex stress conditions. In response to these problems, the aim of this paper is to analyse the effects of different factors on the load-bearing performance of high-strength bolts on the basis of numerical simulations. The mesoscale critical plastic strain (MCEPS) method was used on the model fracture and the accuracy of the model evaluation was verified. The effects of grade, type, diameter and bolt hole clearance on the ductile fracture behaviour of high-strength bolts were investigated. It was found that fully threaded bolts and through-hole clearances can mainly affect the load-bearing properties of high-strength bolts and increase the bolt's fracture-deformation capacity. The load-bearing performance of high-strength bolts under the influence of different factors was also compared with the Eurocode design (EC3) predictions.

1. Introduction

High-strength (HS) bolts play a critical role in various engineering applications, where they are subjected to significant mechanical loads and are expected to maintain structural integrity under extreme condition [1,2]. The good resistance capacity of the bolted connections can effectively ensure the reliability of the structure. However, the fracture of high-strength bolts can have severe consequences, leading to structural failures and potential safety hazards. Therefore, understanding the fracture behaviour of high-strength bolts is of utmost importance for ensuring the reliability and safety of engineering structures.

Accurately evaluating the ultimate capacity of high-strength bolts under composite loads is necessary to ensure the security of bolted connecting zones for the assembled steel structures. However, comprehensive testing is expensive and not realistic for all possible connection designs. Finite element simulation provides an alternative approach to predict bolt fracture without conducting extensive experiments. Numerical modelling of bolted connections utilized various techniques to

capture the elastic, plastic, and failure behaviour of bolts. To accurately simulate bolt fracture, a significant amount of work involves calibrating the computational model with experimental data. Direct experimental calibration has been successful in specific scenarios but often loses accuracy when extended to other loading configurations, particularly in the case of combined tension and shear loading modes.

Seif et al. [3] used an erosion strain criterion to predict shear fracture of bolts. They developed a finite element model of A325 bolts in double shear using a trilinear material model and compared it with the experimental data of Wallaert and Fisher [4]. The stress–strain of the bolts matched the experimental results; however, the model failed to accurately predict the fracture, resulting in non-conservative estimates of failure stress and strain. Mersch et al. [5] employed a geometrically simplified finite element model to predict bolt failure. The fracture was modeled by deleting elements below an equivalent plastic strain threshold, but the result did not correctly predict bolt failure under different loading conditions. Main and Sadek [6] simulated single and double shear failure of bolts and compared the results with experimental

Fig. 1. Bolted connection joints in engineering.

(a) Boundary conditions

Table 1
Geometry dimensions of partially threaded bolts.

	Nut (mm)				Bolt (mm)		
		Diameter	thickness	Pitch	Diameter		
					D_{maj}	D_{min}	D_p
Geometry size	M16	27	14	2.0	16	13.84	14.72
	M20	34	17	2.5	20	17.29	18.38
	M24	36	21	3.0	24	20.76	22.05

Fig. 3. Typical finite element mesh.
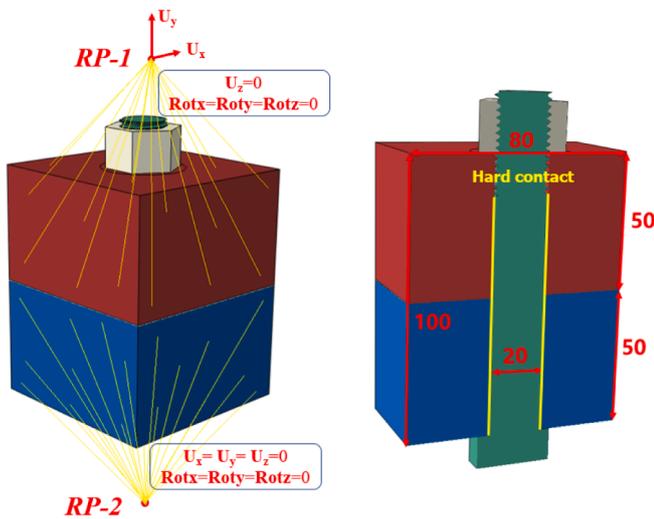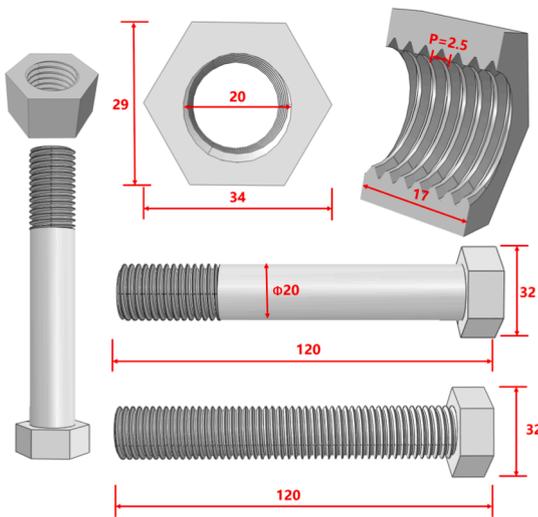
(b) Geometric size

Fig. 2. Boundary condition and geometric size of the model.
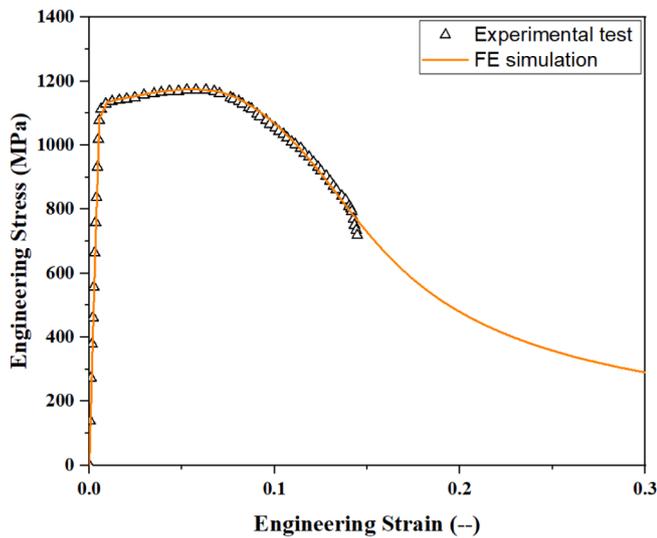
Fig. 4. Engineering stress–strain relationships for grade 10.9 high-strength bolt without consideration of damage.

(a). fully threaded screws
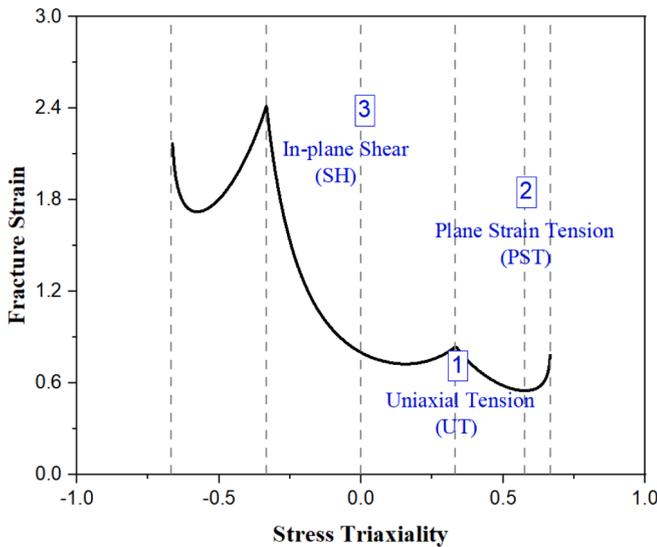
Fig. 5. Relationship between stress triaxiality and fracture strain.

(b). partially threaded bolts

Fig. 6. Validation of the simulated Grade 10.9 bolts.

data. Bolt the bolts and plates were modeled using segmented linear material, and the criterion of failure was simulated by deleting element under erosion strain. This model successfully reflected the force-–displacement characteristics of bolts under double shear, making it one of the few successful examples in predicting bolt shear fracture. Song et al. [7] performed FE modeling of bolts under tension and shear loading conditions, with fracture criterion controlled by the Lee-Wierzbicki model for element removal, where the critical plastic strain is a stress triaxiality-dependent segmented function. The results were compared with the combined tension-shear loading results, and some post-ultimate behaviour had good agreement with the test data, but the accuracy was insufficient for other loading conditions. Fransplass et al. [8,9] simulated the fracture of threads under shear, tension, and shear-tension combined loads, using the Cockroft-Latham critical [10] strain energy criterion to control element deletion, which is a function of the maximum principal stress. However, the load–displacement behaviour was inaccurate throughout the elastic and plastic stages for all three loading directions.

Indeed, several studies have utilized finite element modeling to simulate the fracture behavior of bolts. However, these models often achieve accurate predictions of the load-deformation relationships only in specific states, and when applied to other loading conditions, the results tend to lose their validity. Simply modeling bolt behaviour based on axial loads is insufficient to accurately capture bolt behaviour and ultimate failure point. It is necessary to consider behaviour under combined loads.

This study discussed the calibration of high-strength bolt fracture coefficient based on the uniaxial engineering stress–strain relationship and applied to accurately predict ductile fracture under combined load states, in order to investigate and analyze the ductile fracture behaviour of high-strength bolts. The uncoupled ductile fracture model for high-strength steel was utilized, and the mesoscale failure index was employed as the criterion for element failure in high-strength bolts [11], successfully achieving fracture prediction for tension-shear combined loading conditions. Furthermore, the study considered four interesting parameters of bolt behaviour: Grade, Type (partially or fully threaded bolts), Diameter, and Hole clearance, as influencing factors in

Table 2

Ultimate capacity for various grades of High-strength bolts at different loading modes.

Grade		Tensile-shear displacement ratio (U_y/U_x)								
		∞ (UT)	5	2	1.25	1	0.8	0.5	0.2	0 (SH)
G8.8 (kN)	P_y	250.141	259.265	257.232	255.428	249.586	229.267	169.672	41.597	0
	P_x	0	48.576	61.587	67.718	73.559	91.226	129.650	177.954	191.656
	P_u	250.141	263.776	264.502	264.252	260.200	246.750	213.536	182.751	191.656
	P_0					238.794				
G10.9 (kN)	P_y	315.922	327.426	326.989	316.029	300.956	276.346	188.183	29.790	0
	P_x	0	62.368	96.177	103.305	120.774	151.245	189.823	233.244	241.361
	P_u	315.922	333.313	340.840	332.485	324.285	315.027	267.293	235.139	241.361
	P_0					318.392				
G12.9 (kN)	P_y	341.806	352.293	352.181	349.210	337.245	301.437	190.143	24.518	0
	P_x	0	64.959	87.989	96.233	109.094	140.052	205.438	251.078	264.008
	P_u	341.806	358.232	363.006	362.227	354.451	332.383	279.927	252.272	264.008
	P_0					344.925				
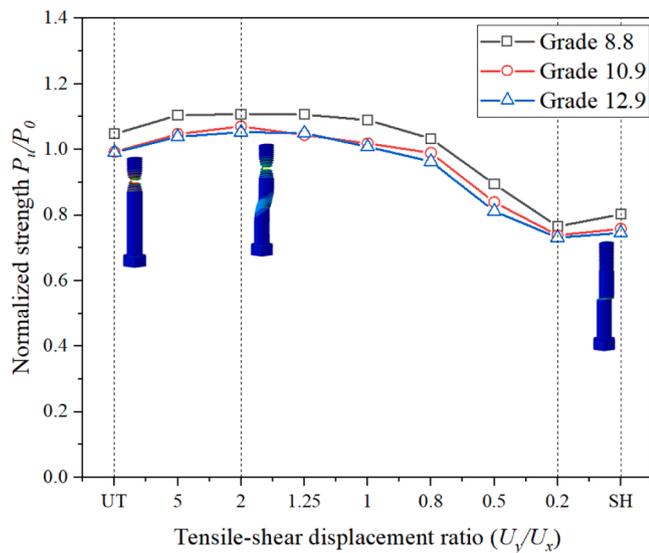
Fig. 7. Bolt-Grade comparison of normalized strength ratio P_u/P_0 for M20 partially threaded bolts.

simulating the complete process of ductile fracture in high-strength bolts. the ultimate strength and deformation behaviour of bolts were analyzed under different loading conditions.

2. Finite element modelling

2.1. Model geometry information

Fig. 1In the setup, a bolt with threads in fixed between two blocks. The lower block restricts displacements and rotations in three directions through a coupled reference point RP-2. The upper block applies axial displacement Uy and tangential displacement Ux to the bolt through constraining the reference point RP-1 of the entire block, allowing for a combine tension-shear loading on the bolt, as shown in Fig. 2(a). It is worth noting that, for ease of describing different combinations of loading states, we refer to Uy/Ux as the applied displacement ratio, which enables loading the bolt with various proportions of tensile-shear states.

The geometric dimensions of the bolt and nut comply with ISO standard specifications [12]. Taking a 120 mm long bolt with a 100 mm threaded portion as an example, using a bolt with a diameter of 20 mm, as shown in Fig. 2(b). The bolt diameter affects the pitch during thread modelling, and the relationship is defined in the international standard ISO 68-1 [13]. For bolts with diameters of 16 mm, 20 mm, and 24 mm,

the pitches are 2.0 mm, 2.5 mm, and 3.0 mm, respectively. The summarized results are presented in Table 1.

Where:D_{maj} is the maximum diameter of the thread, D_{min} is the minimum diameter of the thread, and D_p is the effective diameter of the thread. The cross-sectional area at the thread is calculated from the effective diameter.

2.2. Modelling approach

The model is built based on the tensile test results of grade 10.9 high-strength bolts conducted by Li et al [14]. The mesh element type used is C3D10M, which represents a tetrahedral element with ten nodes, as shown in Fig. 3. The density is 7.8 g/cm3, the Poisson's ratio is 0.3, and the average yield ($f_{0.2\%}$) and ultimate (f_u) stresses are 1013 MPa and 1100 MPa, respectively. The contact surfaces in the model are all defined as hard contact with a penalty function for tangential friction with a coefficient of 0.15. The dynamic explicit solver is employed with a time increment of 1e-5. During loading, the lower clamped block remains stationary, while different displacement constraints are applied to the upper clamped block to achieve tension and shear combination.

The uncoupled phenomenological model [15,16] is used to simulate the fracture behaviour of high-strength bolts, where plastic deformation and fracture are treated as independent processes. The plastic behaviour is calibrated by considering the deformation behaviour of high-strength bolts under axial tension, the true stress-plastic strain relationship is adjusted and the plastic flow curve of the bolt is derived with reference to the engineering stress–strain curve, as shown in Fig. 4. The mesoscale critical equivalent plastic strain criterion proposed by Xin et al. [17-19] is adopted to calibrate fracture paths under different stress states. Specifically, the critical equivalent plastic strain of the element is used as the fracture criterion, which incorporates the three axial stress parameters. The mesoscale critical equivalent Plastic strain (MCEPS) provides a method to calibrate fracture plane parameters solely based on the uniaxial tensile stress state. Fig. 5 shows the calibrated fracture surface for a grade 10.9 high-strength bolt. 3.1.2 Comparisons between FE simulation and test results. In uniaxial tension, the fracture strain is set to 0.84, and the stress triaxiality η is calculated as 0.33. The fracture strain is 0.80, and 0.55 for shear and plane strain tension, separately, corresponding to a stress triaxiality of 0 and $1/\sqrt{3}$ respectively.

Fig. 5 Calibrated result of stress triaxiality and fracture strain for grade 10.9 high-strength bolts. Based on the validated plastic behaviour and fracture parameters, the test results of grade 10.9 high-strength bolts were adopted to validate the applicability of the model for fracture prediction in different loading types. Three loading conditions (uniaxial tension, pure shear, and combined loading with a tension-to-shear ratio of 1) were extracted for finite element comparisons. The simulations ensured consistency in boundary conditions and loading configurations, and the deformation-load curves of the predicted results exhibited good agreement with the test data, as shown in Fig. 6.
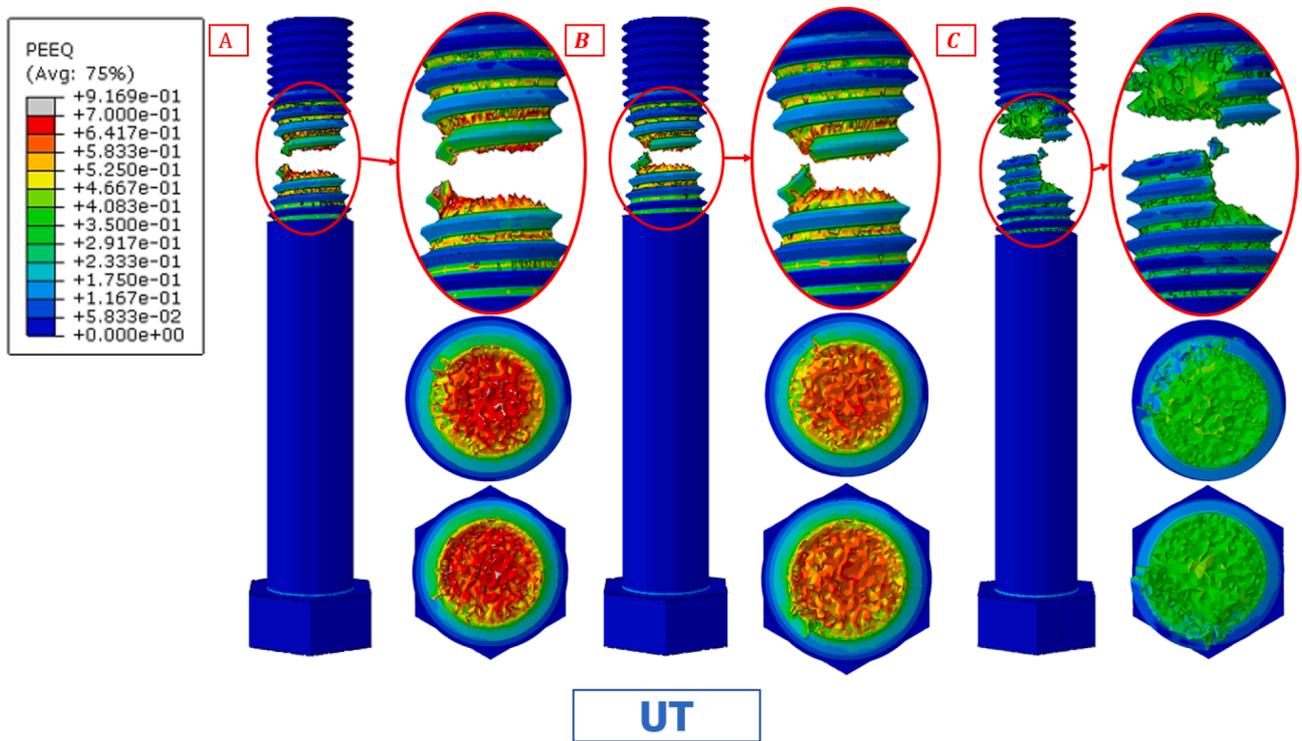
(a) Uniaxial tension ($U_y/U_x=0.0$)
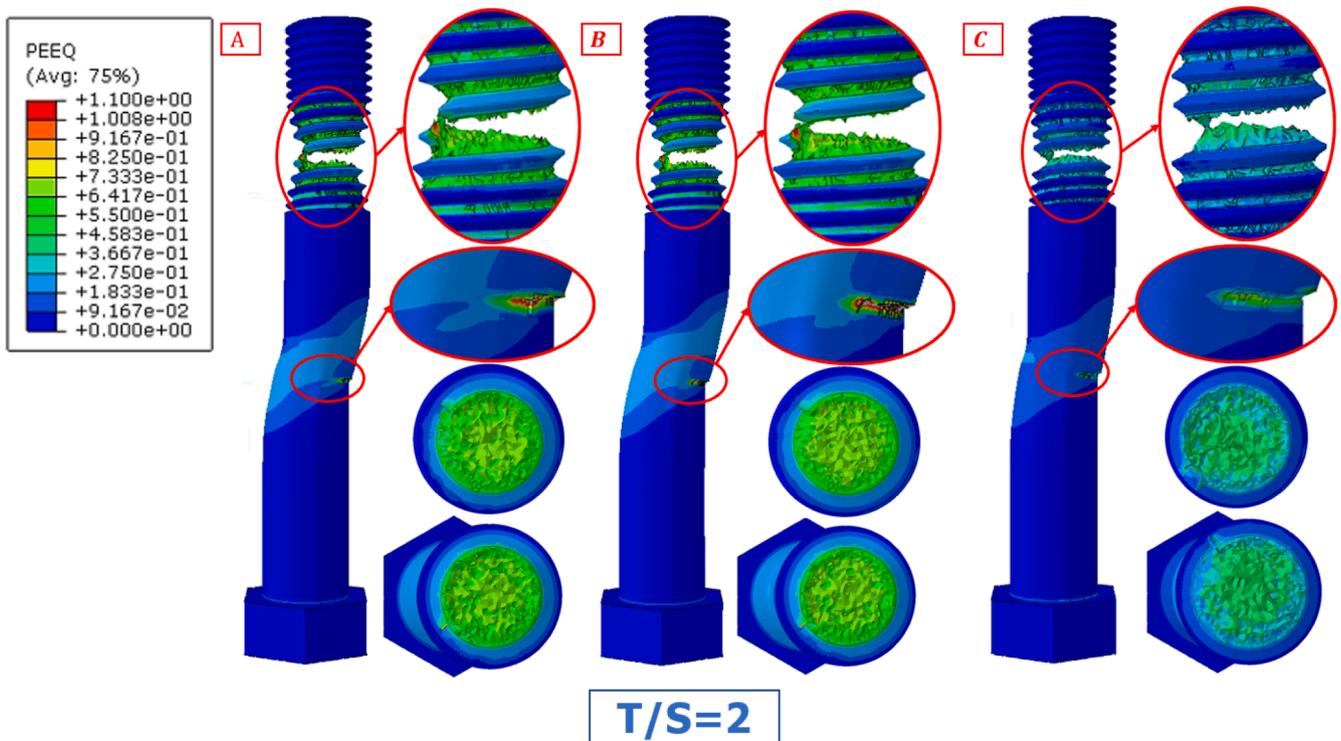
(b) Coupled tension and shear loading for $U_y/U_x=2.0$

Fig. 8. The failure modes of partially threaded M20 bolts, grades 8.8 for *A*, 10.9 for *B* and 12.9 for *C*.
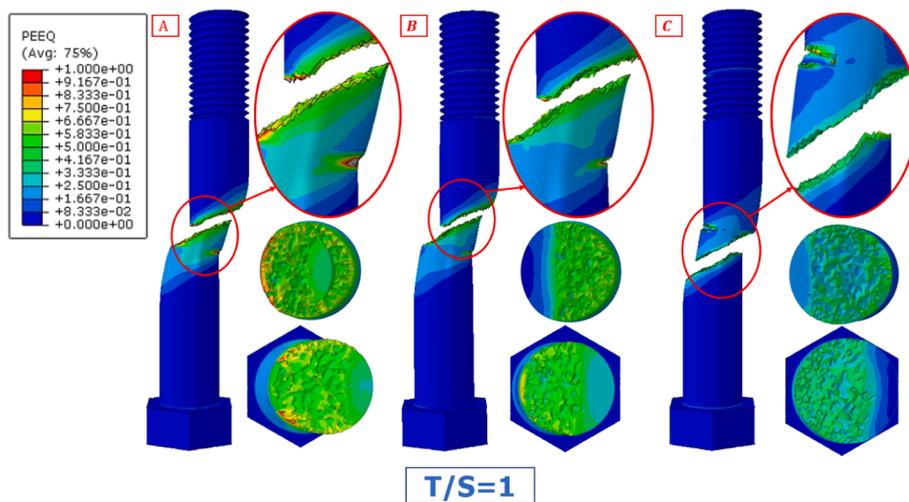
(c) Coupled tension and shear loading for U_y/U_x=1.0
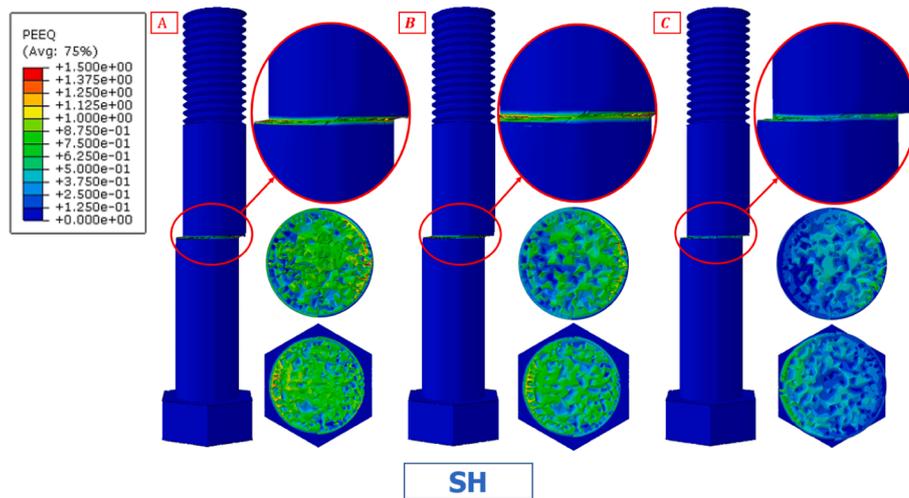
(d) Pure shear (U_y/U_x=∞)

Fig. 8. (*continued*).

Table 3
Simulated result of M16 bolt ultimate capacity.

10.9 bolts		Tensile-shear displacement ratio (U_y/U_x)						
		∞ (UT)	3.73	1.73	1	0.58	0.27	0 (SH)
M16P	P_y	214.503	218.218	216.548	206.844	173.214	128.448	0
	P_x	0	29.142	55.741	65.289	97.933	130.578	163.223
	P_u	214.503	220.156	223.607	216.903	198.982	183.166	163.223
M16S	P_y	190.227	188.102	180.960	165.709	147.983	124.148	0
	P_x	0	20.366	40.732	61.098	81.464	101.830	122.822
	P_u	190.227	189.201	185.488	176.614	168.924	160.568	122.822
P_0(kN)					203.660			

additionally, acceptable consistency in the final fracture morphology of the bolts was also compared under different conditions, this indicates that the model can successfully be applied to simulate the ductile fracture behaviour of high-strength bolts under combined loading conditions.

3. Parametric analysis

With the validated numerical model, this study aims to enhance the understanding of the ductile fracture behaviour of high-strength bolts through a series of parametric investigations. The influence of four practical parameters, including bolt grade, diameter, type, and clearance hole gap, is considered. Based on different applied displacement ratios, the ductile fracture behaviour of high-strength bolts was simulated under nine combinations of loads, ranging from uniaxial tension (Uy/Ux =∞) to pure shear (Uy/Ux = 0).The focus is on analysing the effects of different parameters on deformation and ultimate load-carrying capacity. It is worth noting that in order to facilitate comparison of trends in the ultimate resistance of high strength bolts in various combined conditions, the nominal strength to uniaxial tension P_0 has
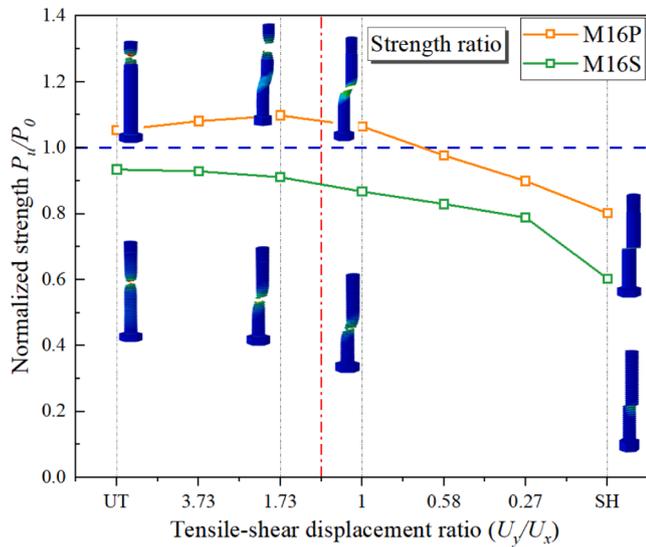
Fig. 9. Bolt-type comparison of normalized strength ratio P_u/P_0 for 10.9 bolts.

been used as a benchmark to normalise the ultimate strength in the different conditions:

$$P_0 = \pi \frac{D_p^2}{4} f_u \qquad (1)$$

3.1. Effects of bolt grade

The effects of bolt grade on the ductile fracture behaviour of high-strength bolts were investigated, considering three grades: Grade8.8, Grade 10.9, and Grade 12.9. The fracture of M20 partially threaded bolt was simulated, and the ultimate resistance of different grades of bolts under various loading conditions was summarized in Table.2. As shown in Fig. 7, the high-strength bolt with higher grade exhibited lower normalised strength.

The failure mode of typical loading conditions was illustrated in Fig. 8. As observed, higher bolt grade exhibited less equivalent plastic strain at fracture. For the uniaxial tension (Fig. 8-a), the deformation

mainly occurred around the threaded zone. For the tensile-dominated tensile-shear coupling loading status (Fig. 8-b), in addition to the fracture surface in the threaded zone that led to catastrophic failure, a small crack is also observed around the middle shank part. For the shear-dominated tensile-shear coupling loading status (Fig. 8-c), an oblique fracture surface is observed at the shank of the bolt. The maximum equivalent plastic strain occurred on both sides of the shank. The maximum plastic strain of grade 8.8 high-strength bolts reached 1.0, and plastic deformation occurred in a large area around the fracture surface, with values tapering along the screw from the fracture to both sides. The plastic deformation of G10.9 occurred around the fracture surface and its distribution area was smaller than that of G8.8. The G12.9 bolt mainly deformed in a narrow area near the fracture surface. For pure shear loading status (Fig. 8-d), a fracture surface perpendicular to the loading direction near the middle of the shank part occurs. The peak value of equivalent plastic strain was 1.500, 1.375, and 1.000 for the bolt grades G8.8, G10.9, and G12.9 respectively.

3.2. Effects of bolt type

The ultimate resistance of partially and fully threaded bolts with grade 10.9 was predicted when exposed to shear-tensile coupling loading in this section. Table.3 showed seven different shear-tensile coupled loads applied to both partially and fully threaded bolts.

Fig. 9 compared the bolt type effect on the ultimate capacity when exposed to shear-tensile coupling loading, The ultimate resistance of partially threaded M16 bolts was 19.6% greater than that of fully threaded M16 bolts. For partially threaded bolts, the normalized strength P_u/P_0 firstly increased and later decreased with the decreasing of displacement ratio and reached the highest value of 1.10 at $U_y/U_x = 1.73$. In addition, the numerical predicted value P_u was lower than the theoretically predicted value when $U_y/U_x > 1.0$ and decreased to 80% in the SH state. The numerical prediction of fully threaded bolts was lower than the theoretical predictions in the full state of tensile-shear coupled loading, and gradually decreased with decreasing of U_y/U_x.

The fracture deformation of high-strength bolts under load in tensile and shear directions was summarized in Fig. 10. As observed that in the tensile direction, the fracture deformation of the fully threaded bolt decreased with the decrease of displacement ratio. While partially threaded bolts showed a tendency to increase and then decrease and
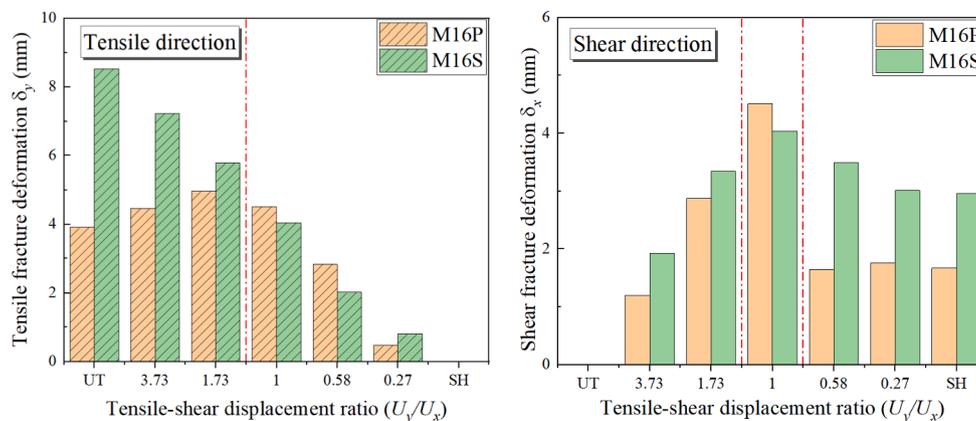
(a). Fracture deformation in tensile direction   (b). Fracture deformation in tensile direction

Fig. 10. Bolt-type comparison of the fracture deformation for 10.9 bolts.
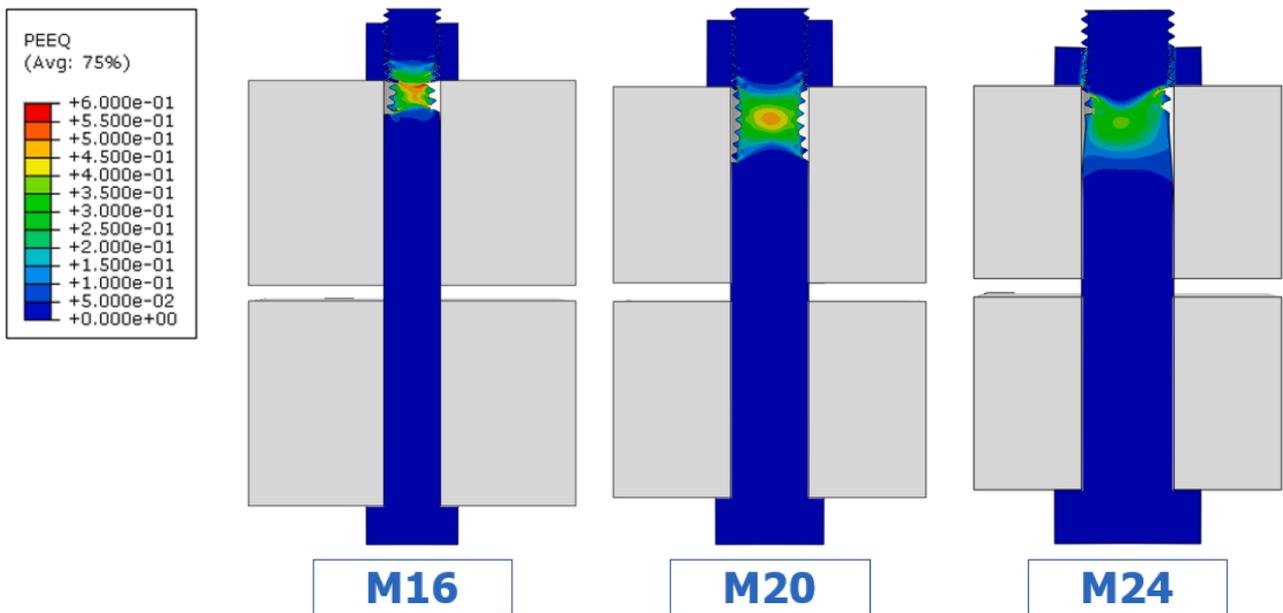
Fig. 11. The equivalent plastic strain in longitudinal sections of 10.9 partially threaded bolts at UT load case, the load is 80% of the resistance.
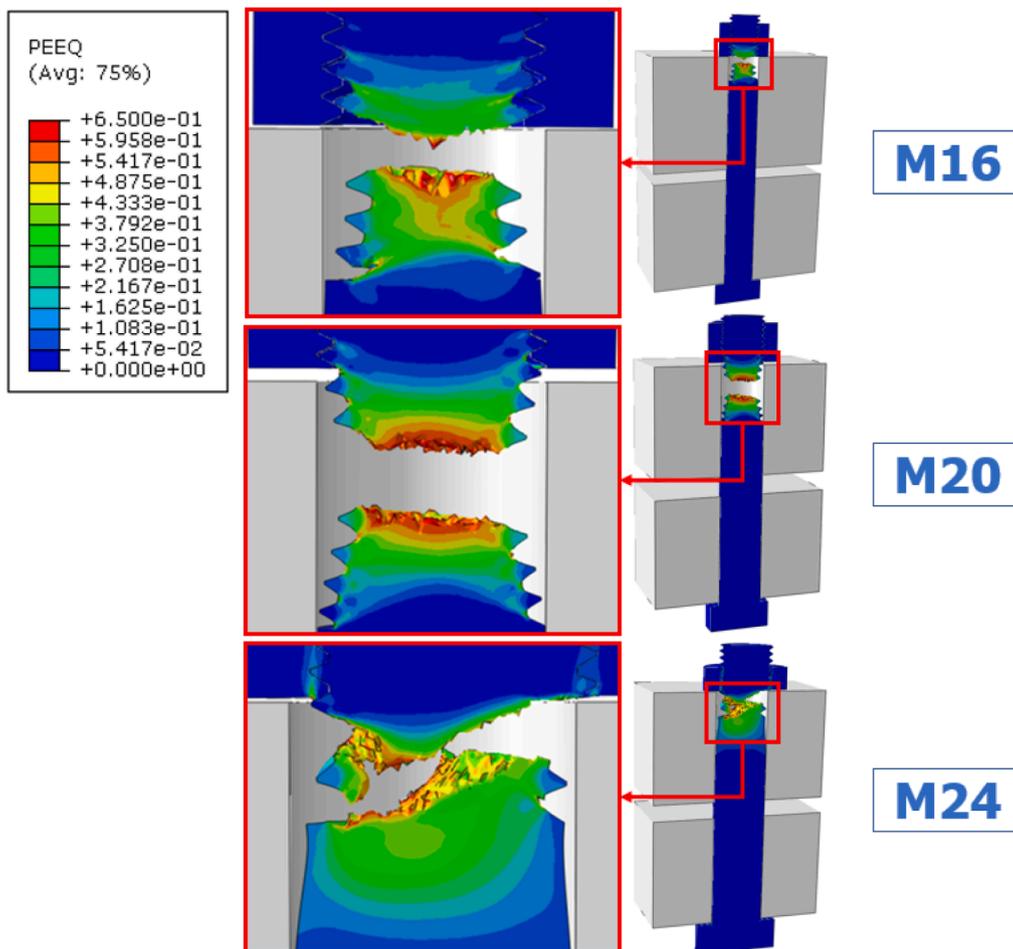
Fig. 12. Longitudinal section of the 10.9 partially threaded bolts with distinct fracture zone.
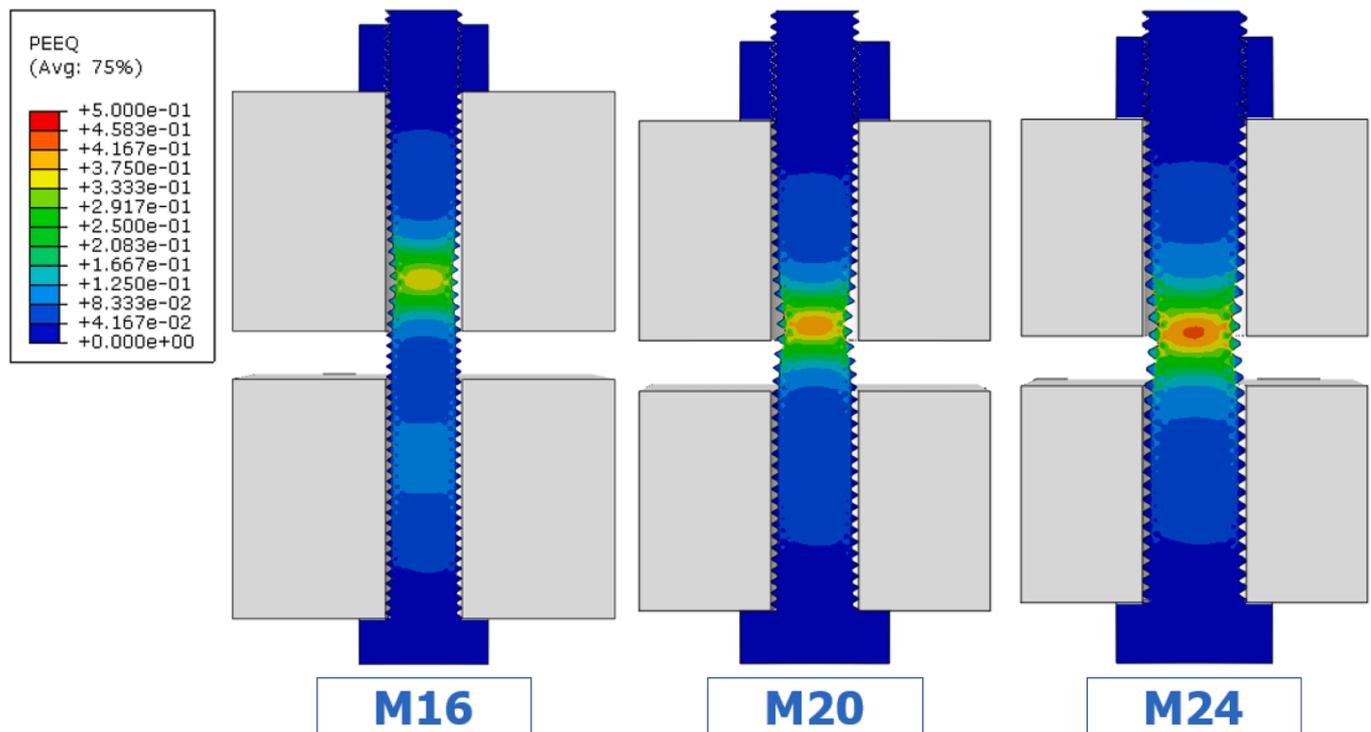
Fig. 13. The equivalent plastic strain in longitudinal sections of 10.9 fully threaded bolts at UT load case, the load is 80% of the resistance.

reached a peak value of 4.96 at $U_y/U_x = 1.73$. both types of bolts showed the deformation behaviour of first increasing and then decreasing in the shear direction, and the deformation value of fully threaded bolts was consistently higher than that of partially threaded bolts except when the ratio of displacement was 1. From Fig. 10-a and Fig. 10-b, the fracture deformation in both axial tension and shear direction of fully threaded bolts is larger than partially threaded bolts.

By observing Fig. 9 and Fig. 10-a, in uniaxial tensile state, although both two bolts fractured at the screw thread, the resistance of the fully threaded bolt was 24 kN lower than that of the partially threaded bolt-even lower than the theoretical ultimate tensile strength-, but the deformation was twice as much as that of the partially threaded. It can be explained that the through-length arrangement of the threads causes the bolt to exhibit greater deformation when subject to uniaxial tension and depletes the bearing capacity to the point where the ultimate resistance is reduced. Which indicated that the resistance of the fully threaded bolt may not perform well in engineering application, and greater deformation will occur when subjected to large external load, making the connection more dangerous.

3.3. Effects of bolt diameter

In this section, three specimens of high strength bolts with diameters of 16 mm, 20 mm and 24 mm are simulated to investigate the effect of bolt diameter on the mechanical behaviour of the bolts. Plastic strain distribution and fracture behaviour of bolts were studied by axial tensile simulations. The equivalent plastic strain distribution of partially threaded bolts at 80% ultimate resistance capacity is shown in Fig. 11. The significant necking was observed at the threads of the three bolts with the peak value of equivalent plastic strain were 0.6, 0.5, and 0.4, respectively. Among them, the distribution of strain deformation for M16 was more concentrated, while was wider for M24. As the block continues to apply displacement, the bolt eventually undergoes ductile fracture at the threaded location, as shown in Fig. 12. For partially threaded bolts, the fracture is essentially perpendicular to the axial

direction. The necking can be observed in the lateral part of the thread. At fracture, the maximum value of equivalent plastic strain reaches 0.65 for M16 and M20 bolts, while 0.60 for M24, which had a limited increase compared to the 80% ultimate resistance in Fig. 11.

Figs. 13 and 14 showed the distribution of equivalent plastic strain and fracture behaviour for the fully threaded bolt respectively. It can be found by comparing the equivalent plastic strain in Fig. 13 that the M24 bolt has the largest value of 0.5, while the M16 had the smallest of the three, which was 0.375. In addition, the largest deformation of bolts with different diameters all occurred inside the screw, which can be interpreted as the bolts being first damaged from the inside when subjected to external loads, which in turn leads to the final fracture failure, as also verified in Fig. 14. M16 bolt had the higher equivalent plastic strain value and more strain areas among the three diameters of bolts, with a peak value of 0.8, while M24 had the least plastic deformation, which was 0.667. This was consistent with the trend of the plastic strain distribution clouds image during fracture for partially threaded bolts. On this basis, analysis of the maximum equivalent plastic strain at 80% ultimate resistance and fracture of the fully threaded bolt revealed a difference of 0.3, indicating that large plastic deformation occurred between the appearance of damage and fracture of the fully threaded bolt.

The ultimate resistance of M20 and M24 bolts at various tensile-shear ratios was summarized in Table 4. The normalized strength of high-strength bolts of different diameters when subjected to coupled shear-tension loads with partial threads was compared in Fig. 15. As observed, the diameter had little effect on the normalized strength of the high-strength bolts, with values for M20 and M24 bolts differing by less than 5%. Fig. 16 showed the fracture deformation in shear and tension directions for partially threaded bolts with diameters of 20 mm and 24 mm, respectively. It can be observed that the fracture deformation of M24P is higher than M20P in both the shear and tensile directions at various tensile-shear ratios (U_y/U_x). This demonstrated that the higher diameter bolts have higher deformation at fracture for partially threaded bolts.
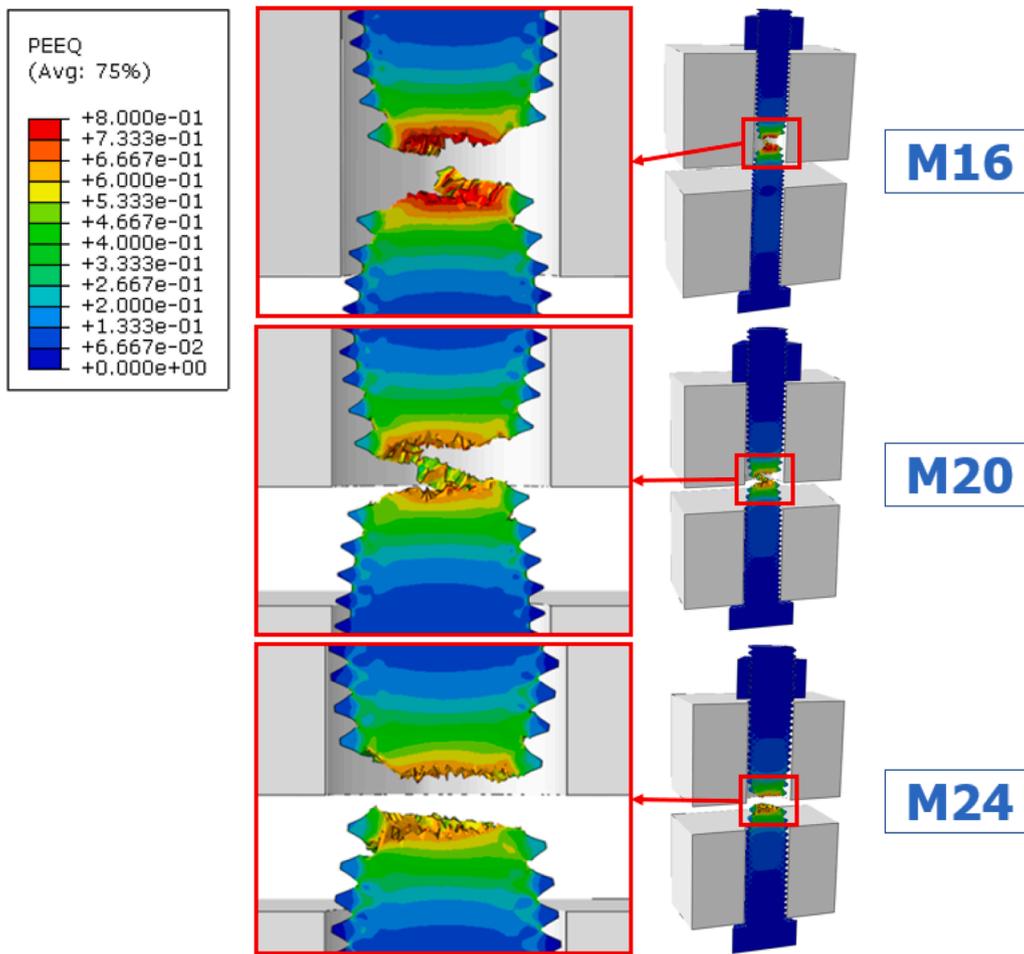
Fig. 14. Longitudinal section of the 10.9 fully threaded bolts with distinct fracture zone.

Fig. 17 compared the ultimate resistance of Grade 10.9 fully threaded bolts. The overall trend of normalized strength Pu/P_0 decreases with decreasing tensile-shear ratio. Expect for the ratio at 0.2, in which the influence of the bolt diameter on the ultimate resistance is not obvious, it can be observed that the line of M24S is above the line of M20S, i.e., the larger diameter bolt has a higher resistance performance for fully threaded bolts. It is worth noting that the normalized strength of a fully threaded bolt is less than 1 in all statuses. On this basis, it is important to ensure the safety of strength in actual engineering use. Fig. 18 compared the fracture deformation for fully threaded bolts with different diameters. Noted that the fracture deformation of M24S was higher than that of M20S in both tensile and shear directions when $U_y/U_x \geq 1$, it means that the use of lager diameter bolt will result in grater displacement of the connection joint, which presents a challenge for structural safety.

Table 4
Simulated result of M20 and M24 bolt ultimate loading capacity.

10.9 bolts			Tensile-shear displacement ratio (U_y/U_x)								
			UT	5	2	1.25	1	0.8	0.5	0.2	SH
Pu(kN)	M20P	P_y	315.922	327.426	326.989	316.029	300.956	276.346	188.183	29.790	0
		P_x	0	62.368	96.177	103.305	120.774	151.245	189.823	233.244	241.361
		P_u	315.922	333.313	340.840	332.485	324.285	315.027	267.293	235.139	241.361
	M24P	P_y	455.281	470.461	483.447	468.342	456.719	423.991	295.929	30.642	0
		P_x	0	76.977	116.752	128.312	143.848	171.205	254.123	337.643	343.669
		P_u	455.281	476.717	497.346	485.601	478.836	457.253	390.068	339.031	343.669
	M20S	P_y	302.239	297.125	296.961	282.359	270.304	250.427	205.175	56.559	0
		P_x	0	11.278	31.838	52.157	69.106	88.508	129.651	176.443	193.982
		P_u	302.239	297.339	304.727	287.136	278.998	265.607	215.349	185.286	193.982
	M24S	P_y	444.683	443.590	431.386	412.108	392.133	359.900	269.003	61.380	0
		P_x	0	15.094	41.302	76.111	105.455	135.006	193.020	259.634	279.019
		P_u	444.683	443.847	433.359	419.077	406.065	384.389	331.088	266.791	279.019
P$_0$(kN)	M20						318.392				
	M24						458.651				
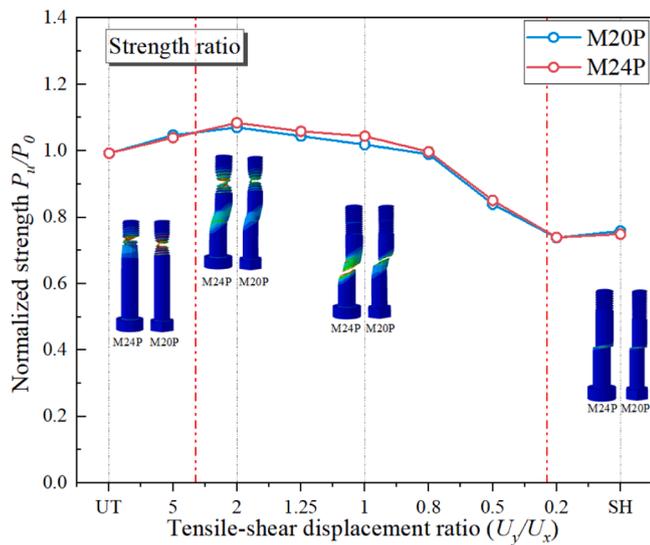
Fig. 15. Diameter comparison of normalized strength ratio P_u/P_0 for 10.9 partially threaded bolts.

3.4. Effects of a bolt hole clearance

Numerical simulations were performed for Grade 10.9, M20 partially and fully threaded bolts with a hole clearance of 1 mm (standard clearance) and 2 mm (increased clearance) in tensile-shear coupled load to analyse the relationship between the gap and load resistance of high-strength bolts, with fitted bolts the control group. Fig. 19 shows the fracture failure of three kinds of gaps under various tensile and shear combinations from uniaxial tension to shear. Where α is the bolt in the fitted bolts, β is the standard clearance, and γ is the increased clearance. As observed, three bolts fractured at the same position at uniaxial tension. When $U_y/U_x = 2$, the fracture site of group α is at the thread, but a large area of plastic deformation is evident out of the shank. β group and γ group did not appear obvious colour changes. When $U_y/U_x = 1.25$, group α bolts have completely entered the failure mode of tensile-shear coupling fracture at the screw out, group β bolts fractured at the screw, besides, there was still necking at the thread, group γ bolt was fractured

at the threads even though there had been deformation in the shear direction. Observing the fracture surfaces of the three groups of bolts in different states, it could be found that the presence of bolt hole clearance delays the fracture type of the bolts from uniaxial tensile to shear damage.

The normalized strength of partially threaded bolts under various statuses with different gaps had been compared, as shown in Fig. 20. The fitted, standard, and increased bolt reached the peak value of 1.07, 1.05, and 1.03 at a tensile-shear ratio of 2, 1, and 0.8, respectively. The ultimate resistance gradually decreased with the increase of bolt hole clearance. In the uniaxial tension state, there is no significant difference in the normalized strength of the three types of bolts because they are not affected by the gap. After deformation in the shear direction occurs, the three lines start to show different tendencies. In the SH state, the bolts are only exposed to shear action, the presence of the gap makes the increased bolt has the lowest strength and fitted bolts have the highest strength. In summary, it is concluded that the existence of the gap delays the peak value of partially threaded bolts, it reduces the maximum ultimate strength, making the bolts more prone to fracture.

Fig. 21 compared the fracture deformation in the tensile and shear directions. In the tensile direction, the fitted bolt reaches a maximum deformation of 9.88 mm at a tensile-shear ratio of 2, standard bolt reaches a maximum of 8.81 mm at 1.25. increased bolt is 7.88 mm at 1.25 and 7.73 mm at 1. In the shear direction, the value of both the fitted and standard bolts reached the peak at the ratio of 1 with fracture deformation of 6.89 mm and 7.33 mm, respectively, while the value of the increased bolt reached a maximum of 8.09 mm at 0.8. Noted that the deformation in the shear direction includes the distance of the gap. it can be found that the gap delays the bolt fracture type (the larger the gap, the smaller the tensile-shear ratio needed to reach the maximum peak fracture deformation). Meanwhile, the gap affected the value of fracture deformation, and an increase in through-hole decreases the value of fracture deformation of the bolt.

Fig. 22 showed the comparison of the normalized strength ratio for fully threaded bolts, the ultimate strengths of the bolts in all three gap states occurred in uniaxial tension and were equal in magnitude. Fitted bolts experienced a sharp decline in bearing strength when the ratio of displacement began to decrease from 1, with a 0.29 drop in normalized strength between 0.2 and 1. Standard bolts experienced a sharp decline after less than 0.8, with a 0.30 drop between 0 and 0.8. The increased bolt decreases at 0.5 with a 0.33 difference between 0 and 0.5. In
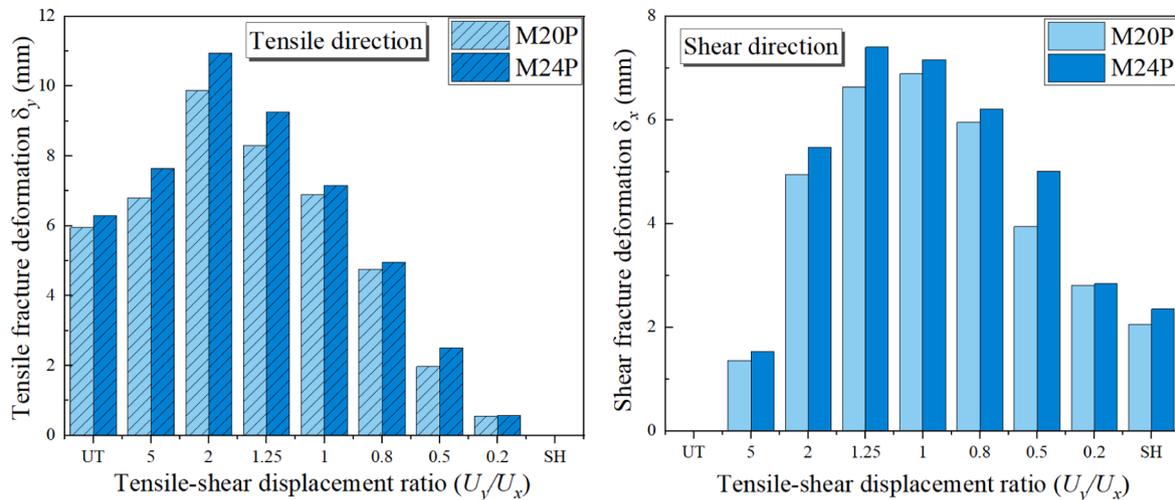
Fig. 16. Diameter comparison of the fracture deformation for 10.8 partially threaded bolts.
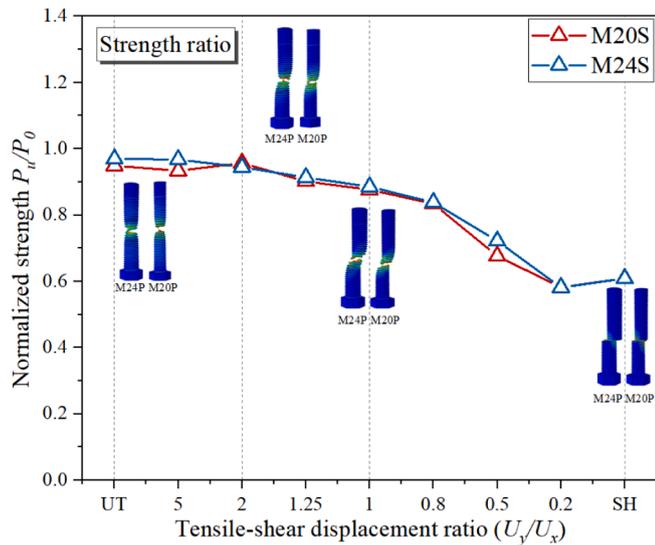
Fig. 17. Diameter comparison of normalized strength ratio P_u/P_0. For 10.9 fully threaded bolts.

addition, in the shear state ($D_y/D_x = 2$), the resistance of high-strength bolts exhibits a decrease with increasing bolt hole clearance. Fig. 23 compared the fracture deformation of fully threaded bolts in the tensile and shear directions. As can be seen in Fig. 23 (a), the value maintained a decreasing trend as the tensile-shear ratio decreased, and the length of fracture deformation in the axial direction became gradually larger as the gap increased. The deformation of the fitted bolt was on average 0.84 larger than standard ones, which was larger than increased ones by 1.54. In the shear direction, the fracture deformation from uniaxial tension to shear showed a tendency to rise and then fall, with the fitted bolt reaching a peak of 7 mm at the ratio of 0.8 and the increased bolt reaching a peak of 9.07 mm at 0.5. In the SH state, the shear deformation of the three bolts was 7.57, 6.29, and 3.17, respectively, which indicated that the increase in bolt gap increases the fracture deformation in the shear direction.
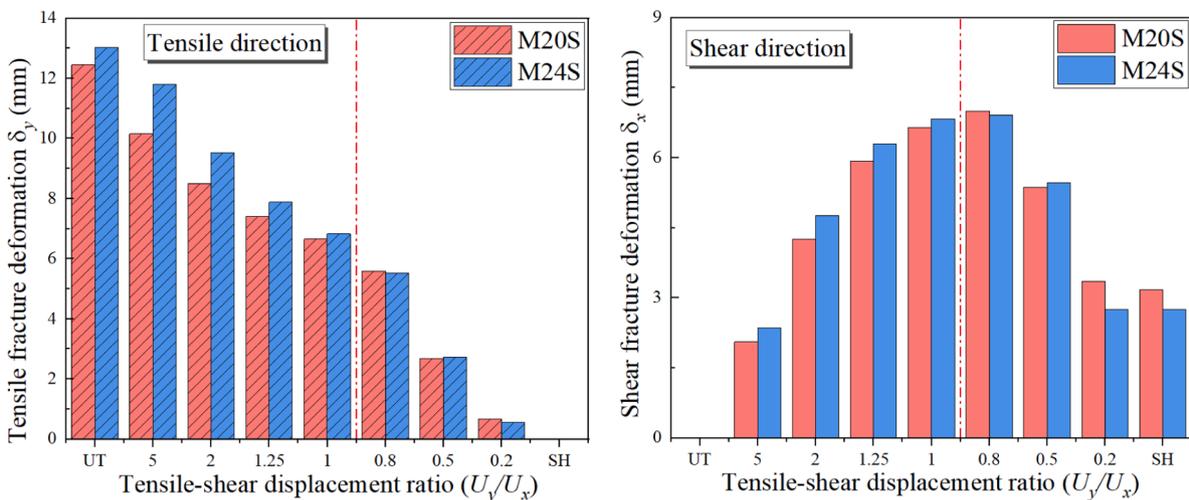
4. Discussion

This study investigated the strength of high-strength bolts under different influencing parameters and compared them with the design recommendations outlined in the European standard Eurocode 3 (2005) [20]. The shear and tension resistance of the structural bolts are defined as below:

$$F_{t,Rd} = \frac{k_2 f_u^b A_s}{\gamma_{M2}} \qquad (2)$$

$$F_{v,Rd} = \frac{\alpha_v f_u^b A}{\gamma_{M2}} \qquad (3)$$

$$\frac{F_{V,Ed}}{F_{V,Rd}} + \frac{F_{t,Ed}}{1.4 F_{t,Rd}} \leq 1.0 \qquad (4)$$

where α_v is the reduction factor for the bolts under shear force and define as 0.5 and 0.6 when the shear plane passes through the threaded and unthreaded bolts shanks, respectively. A and A_s are the equivalent cross-section of the bolt. k_2 is reduction factor defined as 0.9, γ_{M2} is partial safety factor of ultimate resistance.

As observed in Fig. 24, the ultimate load-carrying performance of high-strength bolts under different influencing factors meets the requirements of EC3 (Eurocode 3). The x-axis represents different influencing factors, the y-axis represents the shear strength ratio, and the z-axis represents the tensile strength ratio. Bolt grade and diameter have a slight influence on the load-carrying performance of bolts, where increasing the bolt grade and diameter leads to a decrease in the ultimate load-carrying capacity of high-strength bolts. The load-carrying performance of partially threaded bolts is significantly better than that of fully threaded bolts, with the largest difference observed at a displacement ratio of Uy/Ux≈5. The presence of bolt holes reduces the ultimate load-carrying performance of high-strength bolts under shear loading conditions, with larger holes resulting in lower ultimate strength of the bolts.

5. Conclusion

This study investigated the modeling approach to calibrate the ductile fracture parameters of high-strength bolts from the uniaxial stress–strain relationship. It achieved the simulation of ductile fracture

Fig. 18. Diameter comparison of the fracture deformation for 10.8 fully threaded bolts.
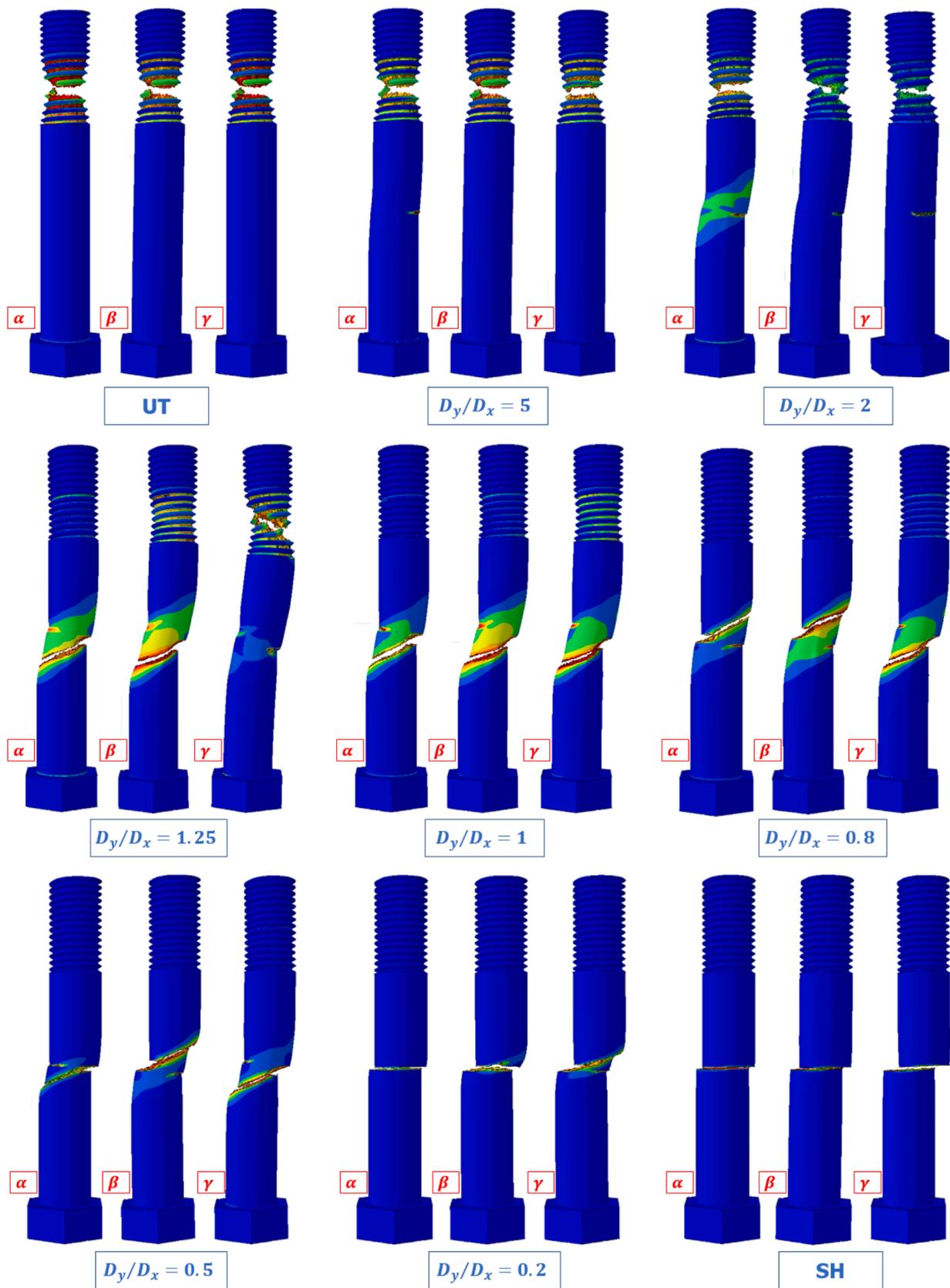
Fig. 19. Comparison of partially threaded bolt fracture surface under various tensile-shear combinations (α. Fitted bolts. β. Standard bolts. γ. Increased bolts.).
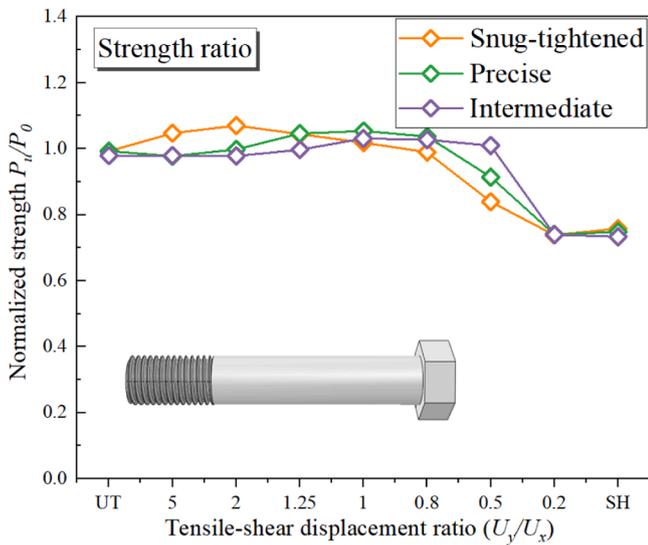
Fig. 20. Bolt hole clearance comparison of normalized strength ratio P_u/P_0 for M20 10.9 partially threaded bolts.

Fig. 22. Bolt hole clearance comparison of normalized strength ratio P_u/P_0 for M20 10.9 fully threaded bolts.

in high-strength bolts under combined tension-shear loading. The influence of bolt grade, type, diameter, and bolt hole clearance on bolt performance under combined loading was studied. A comparison was made with relevant formulas in the European standards, leading to the following conclusions:

1. By utilizing a decoupled phenomenological model, the plastic curve of high-strength bolts was obtained by considering the true stress–strain relationship during uniaxial tension. The fracture surface was calibrated using the mesoscale critical equivalent plastic strain theory. The model accurately simulated the fracture behaviour of high-strength bolts under combined tension-shear loading. Its feasibility was demonstrated by applying the model to other loading conditions.

2. Under combined tensile-shear loading, higher grade high-strength bolts exhibit lower normalized strength and performance lower plastic deformation capacity, making them more prone to fracture.

3. The type of bolt is a key factor that influences the fracture behaviour of bolts. Compared to fully threaded bolts, partially threaded bolts

exhibit higher load-carrying capacity. The absence of threads in the shear plane ensures that partially threaded bolts have higher shear strength. Additionally, the fracture deformations in both tension and shear directions are smaller for partially threaded bolts. This makes partially threaded bolts a safer choice for use in connection joints.

4. When the bolts subject to combined tensile and shear loading, larger diameter bolts exhibit 2%~4% higher nominal strength. As the same time, larger diameter bolts exhibited higher fracture deformation, 9.5% and 5.2% higher for partially and fully threaded bolts, respectively.

5. Bolt hole clearance affects the maximum resistance of the partially threaded bolt, and the peak value decreases by about 2% for every 1 mm increase in gap. For fully threaded bolts, the ultimate resistance drops sharply with the shear displacement increases, the presence of bolt hole clearance slows this trend but reduces the bearing capacity in the shear dominant state.

6. The load-bearing performance results were compared with the relevant formulas in EC3 specifications for different factors, and the simulation results were found to comply with the requirements of the
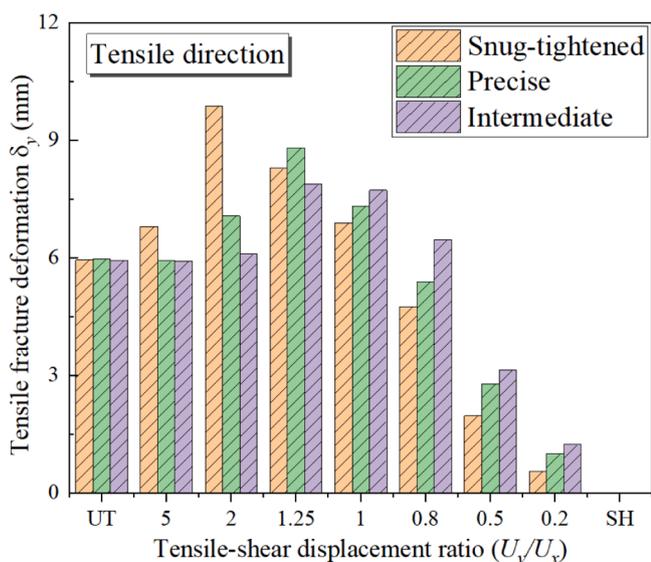
Fig. 21. Bolt hole clearance comparison of the fracture deformation for M20 10.9 partially threaded bolts.
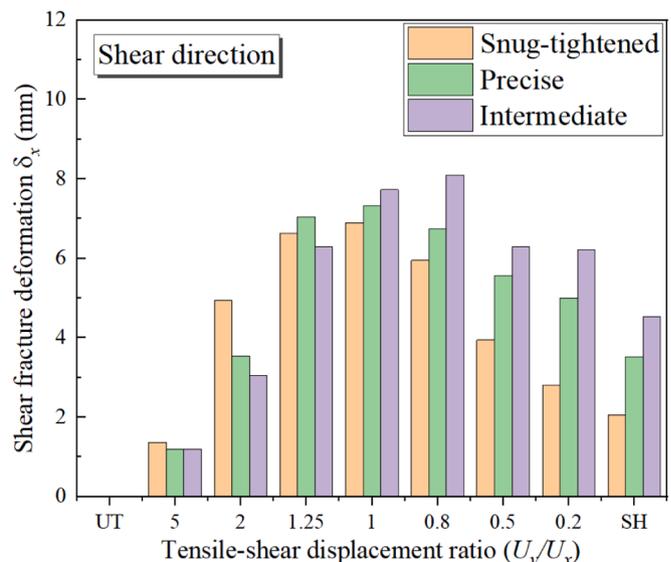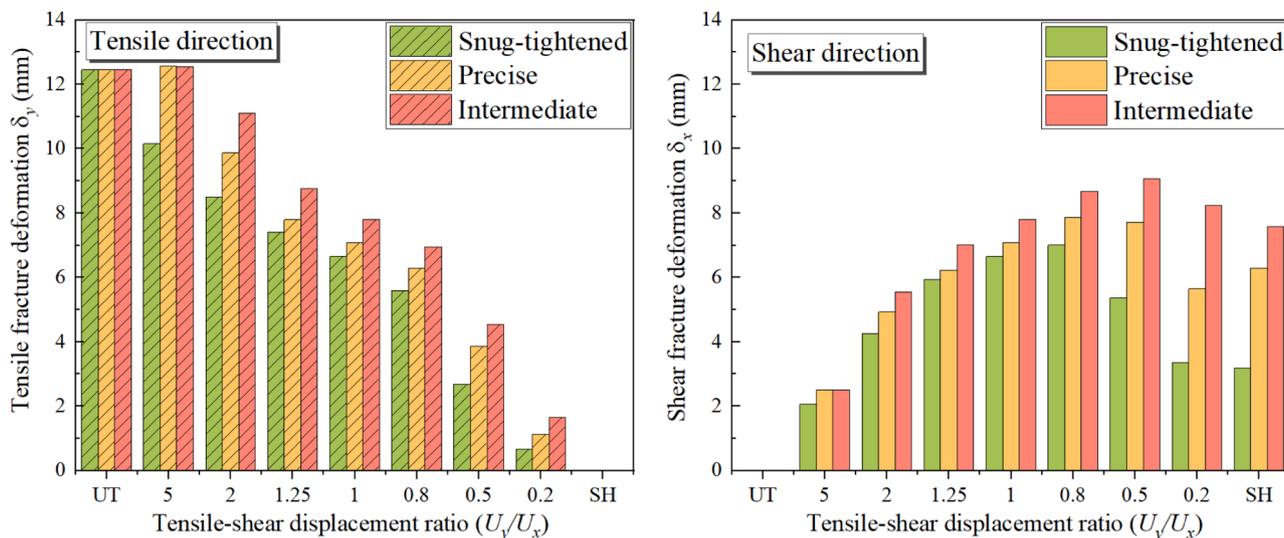
Fig. 23. Bolt hole clearance comparison of the fracture deformation for M20 10.9 fully threaded bolts.

(a)Grade

(b)Type

(C)Diameter

(b)Hole clearance
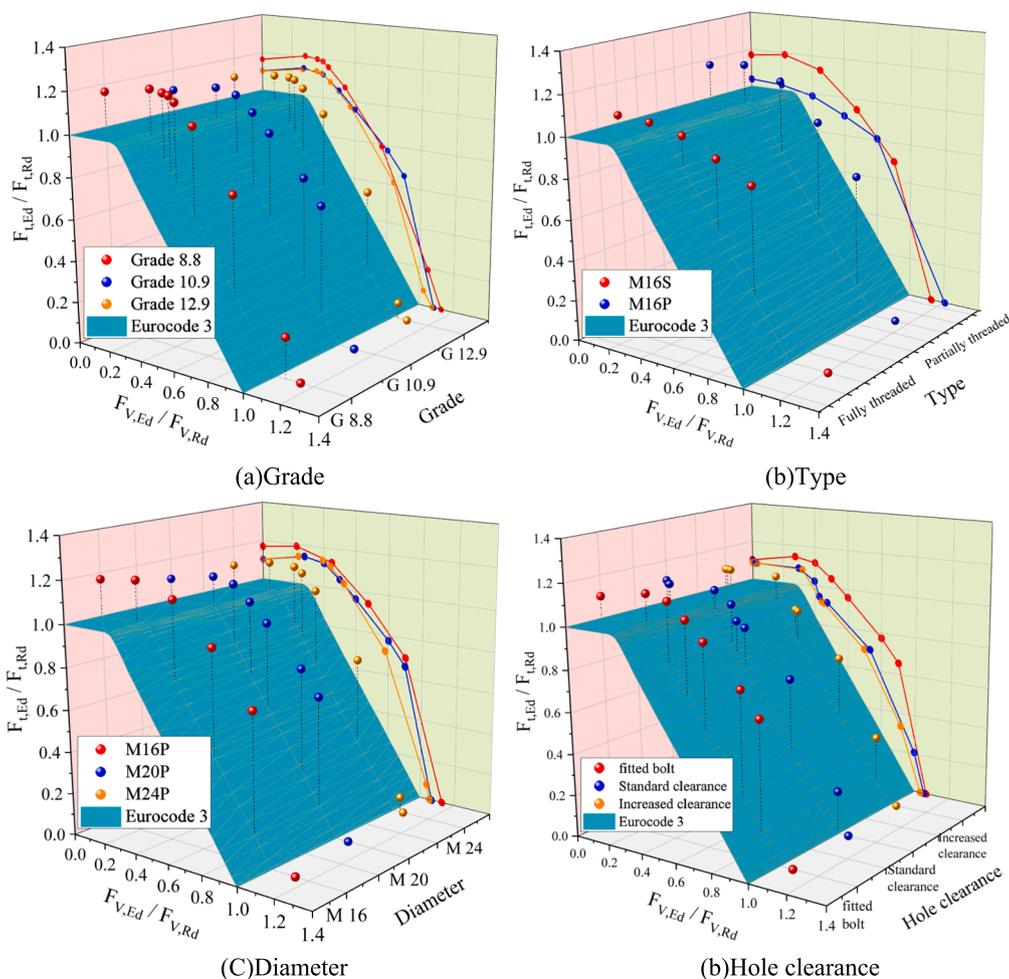
Fig. 24. Comparisons of design strengths between EC3 and simulations under different factors.

specifications. However, it was observed that the specification assessment in the case of combined tension and shear loading is overly conservative, leading to excessive redundancy in design.

Declaration of Competing Interest

The authors declare that they have no known competing financial interests or personal relationships that could have appeared to influence the work reported in this paper.

References

[1] Yang B, Tan KH. Experimental tests of different types of bolted steel beam–column joints under a central-column-removal scenario. Eng Struct 2013;54:112–30.

[2] Yang B, Tan KH. Numerical analyses of steel beam-column joints subjected to catenary action under in-plane loading. J Constr Steel Res 2009;70:1–11.

[3] Seif M, et al. Finite element modeling of structural steel component failure at elevated 631 temperatures. Structure 2016;6:134–45.

[4] Wallaert, J. and J. Fisher, Shear strength of high-strength bolts, in Fritz Laboratory Reports. 1964.

[5] Mersch, J.P., J.A. Smith, and E.P. Johnson. A case study for the low fidelity modeling of threaded fasteners subject to tensile loadings at low and high strain rates. in Proceedings of the ASME 2017 Pressure Vessels and Piping Conference. 2017. Waiikoloa, Hawaii, USA: ASME.

[6] Main J, Sadek F. Robustness of steel gravity frame systems with single-plate shear connections. National Institute of Standards and Technology; 2012.

[7] Song Y, Wang J, Uy B, Li D. Experimental behaviour and fracture prediction of austenitic stainless steel bolts under combined tension and shear. J Constr Steel Res 2020;166:105916.

[8] Fransplass H, Langseth M, Hopperstad OS. Experimental and numerical study of threaded steel fasteners under combined tension and shear at elevated loading rates. Int J Impact Eng 2015;76:118–25.

[9] Fransplass H, Langseth M, Hopperstad OS. Numerical study of the tensile behavior of threaded steel fasteners at elevated rates of strain. Int J Impact Eng 2013;54: 19–30.

[10] Cockroft MG, Latham DJ. Ductility and the workability of metals. J Inst Metals 1968;96:33–9.

[11] Xin H, Correia JAFO, Veljkovic M, Berto F. Fracture parameters calibration and validation for the high strength steel based on the mesoscale failure index. Theor Appl Fract Mech 2021;112:102929.

[12] ISO 262:2:1998, ISO general purpose metric screw threads — Selected sizes for screws, bolts and nuts, 1998.

[13] ISO 68-1:1998 ISO general purpose screw threads – Basic profile – Part 1: Metric screw threads. International Organization for Standardization, 1998.

[14] Li D, Uy B, Wang J, Song Y. Behaviour and design of Grade 10.9 high-strength bolts under combined actions, steel. Compos Struct 2020;35(3):327–41.

[15] Lou Y, Yoon JW, Huh H. Modeling of shear ductile fracture considering a changeable cut-off value for stress triaxiality. Int J Plast 2014;54:56–80.

[16] Lou Y, Huh H, Lim S, Pack K. New ductile fracture criterion for prediction of fracture forming limit diagrams of sheet metals. Int J Solids Struct 2012;49(25): 3605–15.

[17] Xin H, Veljkovic M. Evaluation of high strength steels fracture based on uniaxial stress-strain curves. Eng. Fail. Anal. 2021;120.

[18] Xin H, Li J, Veljkovic M,et al. Evaluating the strength of grade 10.9 bolts subject to multiaxial loading using the micromechanical failure index: MCEPS, STEEL CONSTRUCTION-DESIGN AND RESEARCH, February,2022.

[19] Xin H, Veljkovic M, Correia JAFO, Berto F. Ductile fracture locus identification using mesoscale critical equivalent plastic strain. Fatigue Fract. Eng. Mater. Struct. 2021;44(5):1292–304.

[20] Eurocode 3, Design of Steel Structures, Part 1.8, Design of joints, BS EN 1993-1-8, vol.2005, UK, London, 2005.